QCD FLUX TUBES ACROSS DECONFINEMENT

P. Cea(1,2), L. Cosmai(1), F. Cuteri(3), A. Papa(4)

(1) INFN - Bari
(2) Dipartimento di Fisica Univ. Bari
(3) Institut für Theoretische Physik, Goethe Universität
(4) INFN and Dip. Fisica Univ. Calabria

Introduction

- Reaching a detailed understanding of color confinement is one of the central goals of nonperturbative studies of QCD.

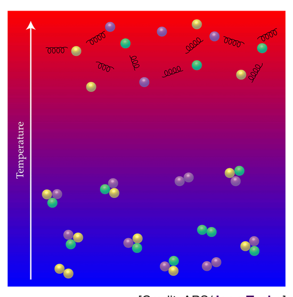
(Credit: APS/Joan Tycko)

- It is known since long that, in lattice numerical simulations, tubelike structures emerge by analyzing the chromoelectric fields between static quarks. Such tubelike structures naturally lead to a linear potential between static color charges and, consequently, to a direct numerical evidence of color confinement.

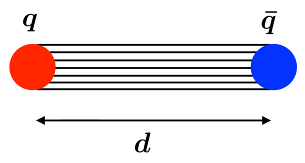

1

How to measure the chromoelectric field on the lattice?

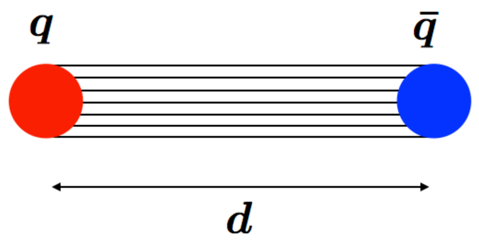

2

To explore on the lattice the field configurations produced by a static quark-antiquark pair —> connected correlation function (*)

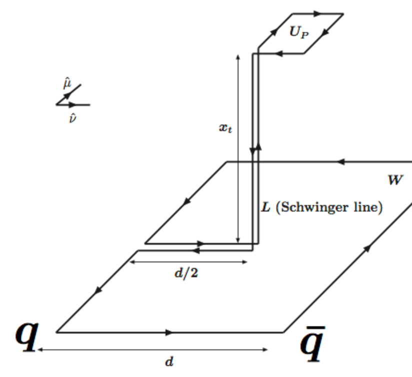

Wilson loop

$T = 0$

$$\rho^{\rm conn}_{W,\mu\nu} = \frac{\langle {\rm tr}\,(W L U_P L^\dagger)\rangle}{\langle {\rm tr}(W)\rangle} - \frac{1}{N}\frac{\langle {\rm tr}(U_P){\rm tr}(W)\rangle}{\langle {\rm tr}(W)\rangle}$$

$U_P = U_{\mu\nu}(x)$ plaquette in the (μ,ν) plane

L Schwinger line

N number of colors

$\rho^{\rm conn}_W \xrightarrow{a\to 0} a^2 g \left(\langle F_{\mu\nu}\rangle_{q\bar q} - \langle F_{\mu\nu}\rangle_0\right)$

$\langle\ \rangle_{q\bar q}$ average in the presence of a static quark-antiquark pair

$\langle\ \rangle_0$ vacuum average (expected to vanish)

field strength tensor $\boxed{F_{\mu\nu}(x) = \frac{1}{a^2 g}\,\rho^{\rm conn}_{W,\mu\nu}(x)}$

(*) Di Giacomo, Maggiore, Oleínik , NPB347(1990)441
Skala, Faber, Zach, NPB494(1997)293
Kuzmenko, Simonov, PLB494(2000)81
Di Giacomo, Dosch, Shevchenko, Simonov, Phys.Rept.372(2002)319

3

Polyakov loop correlator at T≠0

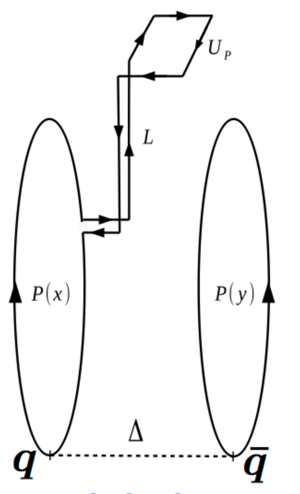

Polyakov loop

$T \neq 0$

$$\rho^{\rm conn}_{P,\mu\nu} = \frac{\langle {\rm tr}\,(P(x) L U_P L^\dagger)\,{\rm tr}\,P^\dagger(y)\rangle}{\langle {\rm tr}\,(P(x))\,{\rm tr}\,(P^\dagger(y))\rangle} - \frac{1}{N}\frac{\langle {\rm tr}\,(P(x))\,{\rm tr}\,(P^\dagger(y))\,{\rm tr}\,(U_P)\rangle}{\langle {\rm tr}\,(P(x))\,{\rm tr}\,(P^\dagger(y))\rangle}$$

$\boxed{F_{\mu\nu}(x) = \frac{1}{a^2 g}\,\rho^{\rm conn}_{P,\mu\nu}(x)}$

4

SU(3) pure gauge T=0 (P.Cea, L.C., F. Cuteri, A.Papa, arXiv:1702.06437)

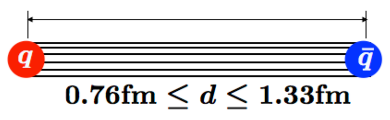

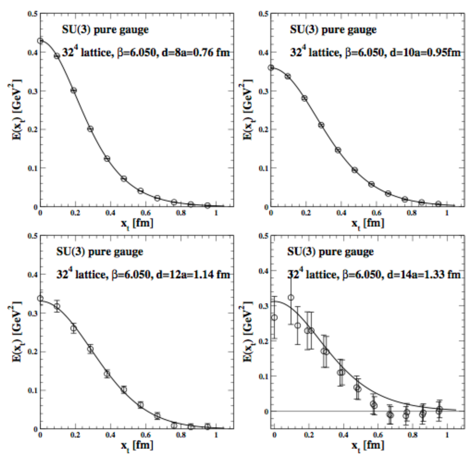

- falloff of the chromoelectric field along the transverse direction
- almost constant transverse size of the flux tube independent of the distance between the sources

5

(2+1) flavors (HISQ fermions)

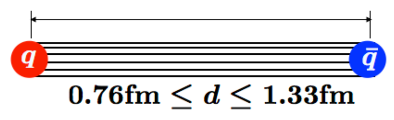

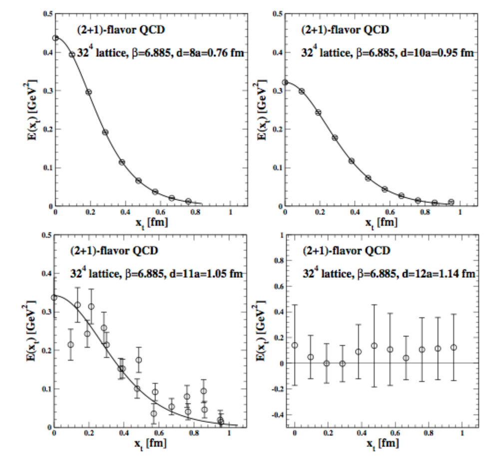

- falloff of the chromoelectric field along the transverse direction
- almost constant transverse size of the flux tube independent of the distance between the sources (comparable with pure gauge)

string breaking at d=1.14 fm ?
(agreement with Bali et al., arXiv:hep-lat/0505012; Koch et al., arXiv:1511.04029)

6

The longitudinal chromoelectric field

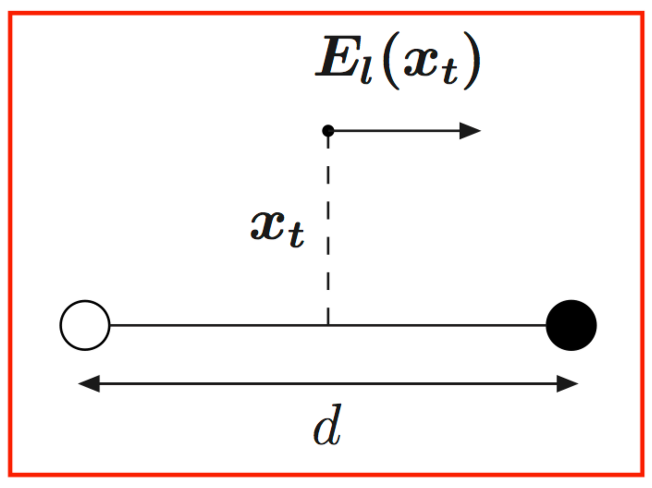

7

LATTICE SETUP

- lattice sizes: 40^3 x 10, 48^3 x 12
- smoothing of the gauge configurations: several APE smearings for spatial links, one HYP smearing for temporal links
- scale setting: (Edwards, Heller, Klassen, Nucl. Phys. B517 (1998) 377)

$$\boxed{(a\sqrt{\sigma})\,(g) = f_{SU(3)}(g^2)\,\{1 + 0.2731\,\hat a^2(g) - 0.01545\,\hat a^4(g) + 0.01975\,\hat a^6(g)\}\,/0.01364}$$

$$\hat a(g) = \frac{f_{SU(3)}(g^2)}{f_{SU(3)}(g^2(\beta=6))} \qquad \beta = \frac{6}{g^2}, \quad 5.6 \le \beta \le 6.5$$

$$\sqrt{\sigma} = 420\ {\rm MeV}$$

$$f_{SU(3)}(g^2) = (b_0 g^2)^{-b_1/2b_0^2}\exp\left(-\frac{1}{2b_0 g^2}\right) \qquad b_0 = \frac{11}{(4\pi)^2}, \quad b_1 = \frac{102}{(4\pi)^4}$$

- # of measurements for each value of the gauge coupling: 3k to 8k (every 10 trajectories)
- **MILC** code (suitably modified to measure the chromoelectric field)

8

The flux tube is almost completely formed by the longitudinal chromoelectric field

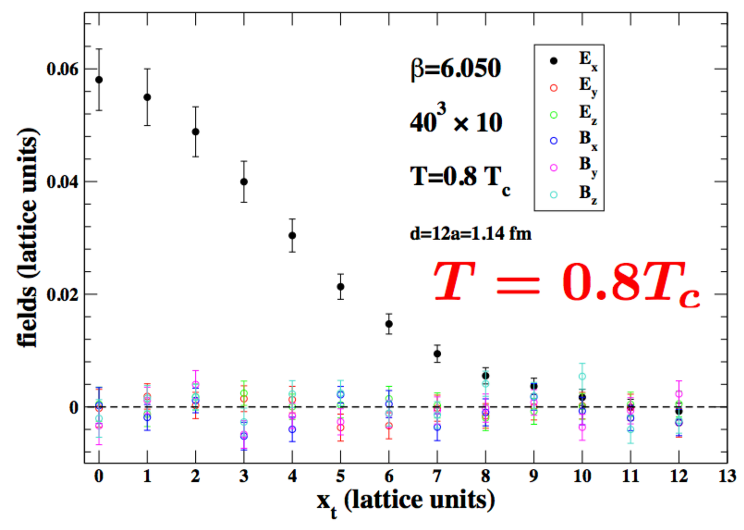

9

check continuum scaling

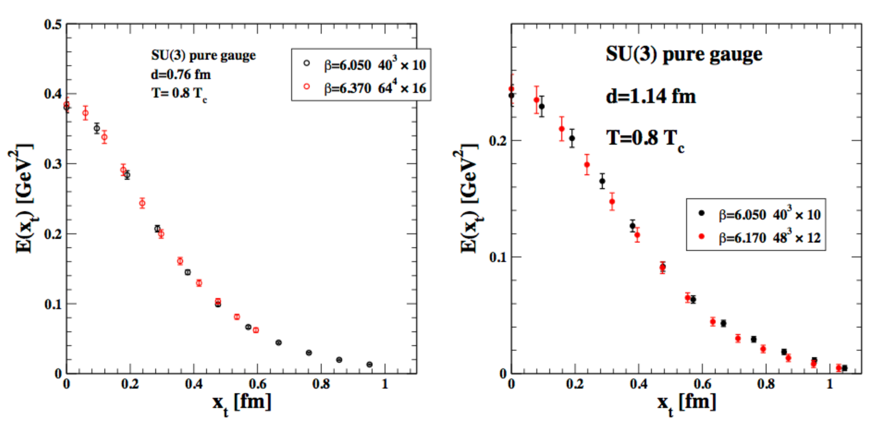

- The continuum scaling is reached at least for β=6.050
- The smoothing procedure is robust: if the smearing had corrupted the physical signal it wold be quite unlikely to obtain such a nice scaling

10

The flux tube shape up to $x_t = 0$

J.R. Clem, J. Low Temp. Phys. 18 (1975) 427

Variational model for the magnitude of the normalised order parameter of an isolated vortex

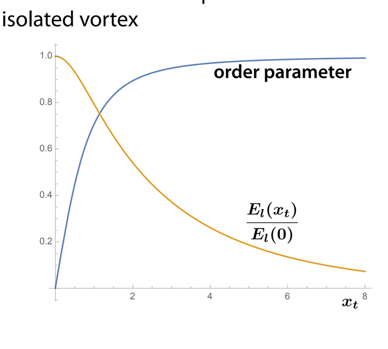

Analytic expression for the magnetic field and supercurrent density that solve Ampere's law and the Ginzburg-Landau equation.

$$\boxed{E_l(x_t) = \frac{\phi}{2\pi}\frac{\mu^2}{\alpha}\frac{K_0((\mu^2 x_t^2 + \alpha^2)^{1/2})}{K_1(\alpha)}}$$

$\mu = \frac{1}{\lambda}, \quad \frac{1}{\alpha} = \frac{\lambda}{\xi_v}$

λ London penetration length

ξ_v variational core radius

ξ coherence length

κ Ginzburg – Landau parameter

$\kappa = \frac{\lambda}{\xi} = \frac{\sqrt{2}}{\alpha}\left[1 - K_0^2(\alpha)/K_1^2(\alpha)\right]^{1/2}$

Analyze lattice data for the flux tubes by exploiting the Clem fit analytic expression for the transverse behaviour of the color electric field.

P. Cea, L.C., A.Papa, Phys. Rev. D86 (2012)054501

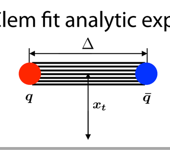

11

the longitudinal field across deconfinement with Clem fit

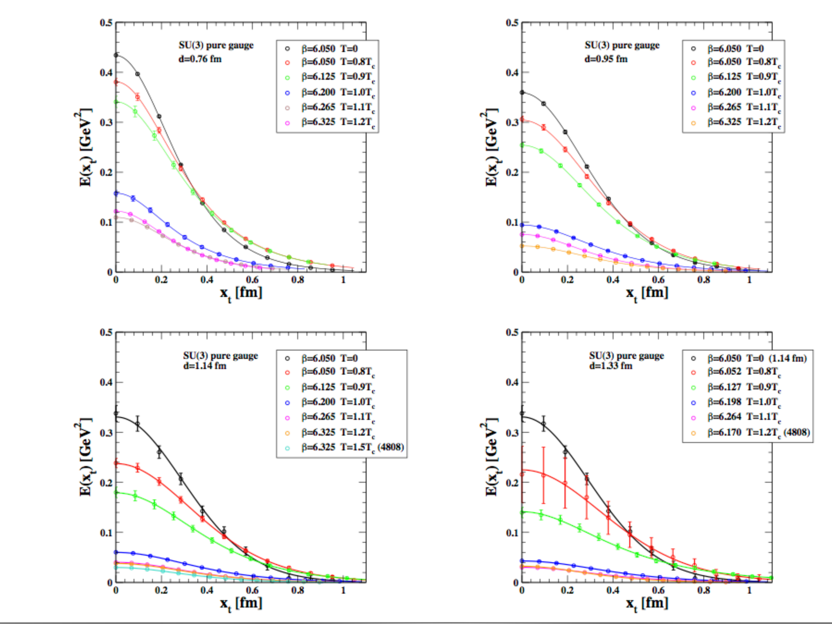

12

PARAMETERS FROM THE CLEM FIT

L_s	L_t	beta	a (fm)	distance (lattice)	distance (fm)	T/T_c	phi	error	lambda (fm)	error	csi (fm)	error	sqrt (w^2) (fm)	error	sqrt(epsilon)/phi (GeV)	error
32	32	6.050	0.0952	14	1.332232	0.00	5.000	0.292	0.169	0.016	0.715	0.335	0.512	0.114	0.117	0.030
40	10	6.052	0.0949	14	1.327978	0.80	5.317	1.108	0.158	0.267	1.520	2.604	0.589	1.308	0.099	0.229
40	10	6.127	0.0844	16	1.350063	0.90	4.400	0.440	0.344	0.097	0.426	0.473	0.825	0.258	0.078	0.027
40	10	6.198	0.0759	18	1.365672	1.00	0.971	0.023	0.207	0.024	0.798	0.401	0.614	0.086	0.098	0.015
40	10	6.264	0.0690	19	1.310212	1.10	0.583	0.004	0.337	0.025	0.777	0.362	0.563	0.023	0.106	0.005
48	8	6.170	0.0791	17	1.344381	1.20	0.481	0.002	0.181	0.004	0.845	0.364	0.562	0.014	0.106	0.003

L_s	L_t	beta	a (fm)	distance (lattice)	distance (fm)	T/T_c	phi	error	lambda (fm)	error	csi (fm)	error	sqrt (w^2) (fm)	error	sqrt(epsilon)/phi (GeV)	error
32	32	6.050	0.0952	12	1.141913	0.00	5.218	0.371	0.143	0.041	0.983	0.428	0.488	0.140	0.120	0.035
40	10	6.050	0.0952	12	1.141913	0.80	5.111	0.219	0.164	0.050	1.210	0.533	0.571	0.225	0.103	0.043
40	10	6.125	0.0846	14	1.184918	0.90	4.192	0.262	0.221	0.066	0.732	0.454	0.634	0.231	0.095	0.038
40	10	6.200	0.0756	15	1.134721	1.00	1.245	0.019	0.215	0.015	0.639	0.376	0.603	0.050	0.101	0.009
40	10	6.265	0.0689	17	1.170625	1.10	0.708	0.005	0.189	0.005	0.656	0.345	0.547	0.018	0.110	0.004
40	10	6.325	0.0633	18	1.139092	1.20	0.683	0.003	0.178	0.004	0.587	0.320	0.510	0.012	0.119	0.003
48	8	6.325	0.0633	18	1.139092	1.50	0.466	0.001	0.149	0.002	0.688	0.298	0.461	0.009	0.129	0.003
48	12	6.170	0.0791	14	1.107137	0.80	4.750	0.261	0.142	0.068	1.462	0.796	0.538	0.339	0.108	0.071

L_s	L_t	beta	a (fm)	distance (lattice)	distance (fm)	T/T_c	phi	error	lambda (fm)	error	csi (fm)	error	sqrt (w^2) (fm)	error	sqrt(epsilon)/phi (GeV)	error
32	32	6.050	0.0952	10	0.951594	0.00	5.287	0.109	0.146	0.017	0.859	0.331	0.479	0.069	0.123	0.019
40	10	6.050	0.0952	10	0.951594	0.80	5.507	0.132	0.184	0.023	0.722	0.361	0.549	0.084	0.109	0.018
40	10	6.125	0.0846	11	0.931007	0.90	4.838	0.104	0.219	0.019	0.535	0.361	0.591	0.061	0.104	0.061
40	10	6.200	0.0756	13	0.983425	1.00	1.738	0.025	0.217	0.013	0.518	0.354	0.583	0.042	0.106	0.042
40	10	6.265	0.0689	14	0.964044	1.10	1.095	0.005	0.197	0.003	0.440	0.312	0.521	0.009	0.119	0.002
40	10	6.325	0.0633	15	0.949243	1.20	0.868	0.004	0.180	0.004	0.506	0.307	0.499	0.012	0.122	0.003

L_s	L_t	beta	a (fm)	distance (lattice)	distance (fm)	T/T_c	phi	error	lambda (fm)	error	csi (fm)	error	sqrt (w^2) (fm)	error	sqrt(epsilon)/phi (GeV)	error
32	32	6.050	0.0952	8	0.761275	0.00	5.143	0.039	0.164	0.005	0.472	0.283	0.458	0.017	0.133	0.005
40	10	6.050	0.0952	8	0.761275	0.80	6.201	0.129	0.249	0.017	0.308	0.331	0.596	0.045	0.108	0.009
40	10	6.125	0.0846	9	0.761733	0.90	5.941	0.194	0.251	0.028	0.337	0.344	0.610	0.077	0.105	0.015
40	10	6.200	0.0756	10	0.756481	1.00	2.061	0.086	0.231	0.029	0.253	0.298	0.543	0.076	0.119	0.076
40	10	6.265	0.0689	11	0.757463	1.10	1.359	0.017	0.200	0.008	0.326	0.289	0.501	0.023	0.126	0.006
40	10	6.325	0.0633	12	0.759395	1.20	1.324	0.020	0.190	0.009	0.293	0.270	0.472	0.024	0.134	0.024
64	16	6.370	0.0595	13	0.773170	0.80	6.554	0.490	0.271	0.046	0.271	0.342	0.631	0.115	0.104	0.021

width of the flux tube:

$$\boxed{\sqrt{w^2} = \sqrt{\frac{\int d^2x_t\, x_t^2 E_l(x_t)}{\int d^2x_t\, E_l(x_t)}} = \sqrt{\frac{2\alpha}{\mu^2}\frac{K_2(\alpha)}{K_1(\alpha)}}}$$

energy in the flux tube per unit length:

$$\varepsilon = \int d^2x_t \frac{E_l(x_t)^2}{2} = \frac{\phi^2}{8\pi}\mu^2\left(1 - \left(\frac{K_0(\alpha)}{K_1(\alpha)}\right)^2\right)$$

$$\frac{\sqrt{\varepsilon}}{\phi} = \sqrt{\frac{\mu^2}{8\pi}\left(1 - \left(\frac{K_0(\alpha)}{K_1(\alpha)}\right)^2\right)}$$

13

across deconfinement

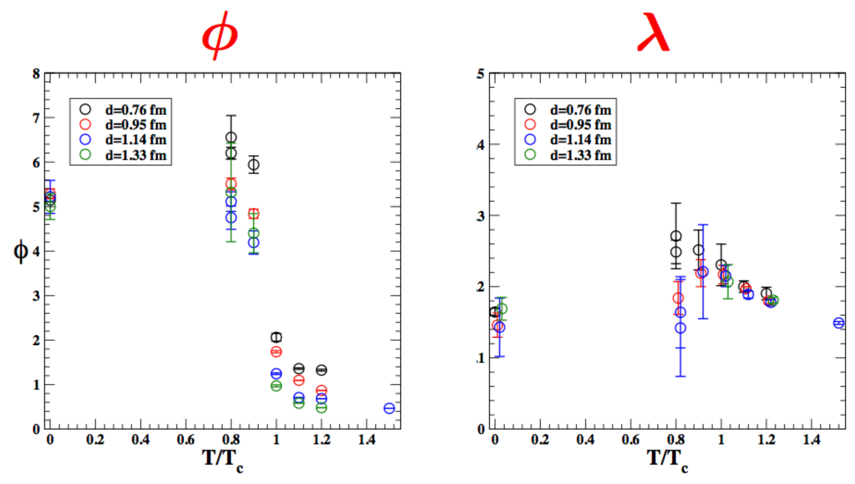

phi drops down across the phase transition

lambda almost constant across the phase transition

14

across deconfinement (cont'd)

$$\sqrt{w^2} = \sqrt{\frac{\int d^2x_t\, x_t^2 E_l(x_t)}{\int d^2x_t\, E_l(x_t)}} \qquad \frac{\sqrt{\varepsilon}}{\phi} = \frac{\sqrt{\int d^2x_t \frac{E_l(x_t)^2}{2}}}{\phi}$$

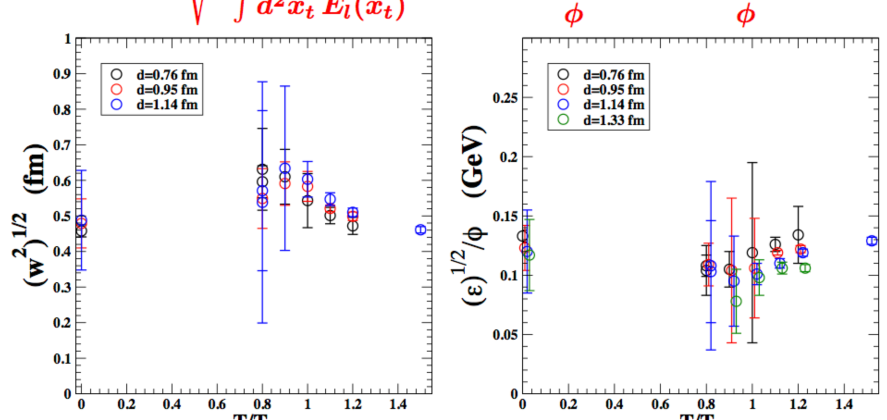

almost constant across the phase transition

almost constant across the phase transition

15